DUST ECHOES FROM GAMMA-RAY BURSTS

ANN A. ESIN[1] AND ROGER BLANDFORD

California Institute of Technology, MS 130-33, Pasadena, CA 91125; aidle@tapir.caltech.edu, rdb@tapir.caltech.edu

ABSTRACT

The deviation from the power-law decline of the optical flux observed in GRB 970228 and GRB 980326 has been used recently to argue in favor of the connection between gamma-ray bursts and supernovae. We consider an alternative explanation for this phenomenon, based on the scattering of a prompt optical burst by 0.1 $M_{\odot}$ dust located beyond its sublimation radius 0.1–1 pc from the burst. In both cases, the optical energy observed at the time of the first detection of the afterglow suffices to produce an echo after ~20–30 days, as observed. Prompt optical monitoring of future bursts and multiband photometry of the afterglows will enable us to test simple models of dust reprocessing quantitatively and to predict source redshift.

Subject headings: dust, extinction — gamma rays: bursts

1. INTRODUCTION

The relationship between gamma-ray bursts (GRBs) and supernovae has become increasingly interesting over the past year. Although exploding massive stars have long been considered as possible progenitors of GRBs (e.g., Woosley 1993), no evidence existed to support these theories until observations of the afterglow of GRB 980425 suggested an association of the burst with an unusual supernova, SN 1998bw (Galama et al. 1998b; Kulkarni et al. 1998). This event prompted reevaluation of the optical afterglow light curves of two other bursts, GRB 970228 and GRB 980326, which showed a deviation from the power-law decline expected if the emission is due to synchrotron radiation from electrons accelerated by the blast wave (Galama et al. 1997, 1998a; Castander & Lamb 1999; Fruchter et al. 1999; Bloom et al. 1999). In both cases, a significant excess emission was observed around ~30 days after the gamma-ray burst, with simultaneous reddening of the spectrum. Bloom et al. (1999), Reichart (1999), and Galama et al. (2000) attribute this excess to the emission from an underlying supernova event.

The relationship of GRBs to supernova (SN) explosions is a question of great importance since it provides a powerful clue to the fundamental nature of these objects. However, the evidence presented so far is circumstantial—the association of GRB 980425 with SN 1998bw is unproven, and the excess emission seen from GRB 970228 and GRB 980326 is based on relatively few actual measurements—and possible alternative explanations need to be seriously considered, if only to strengthen the case for the SN explanation. In this spirit, Waxman & Draine (2000) suggested that the red excess emission observed in GRB 970228 and GRB 980326 is due to dust in the vicinity of the burst progenitor absorbing and then reradiating the optical/UV flash observed shortly after the recent GRB 990123 (Akerlof et al. 1999) and generally attributed to the reverse shock that propagates into the fireball ejecta (Mészáros, Rees, & Papathanassiou 1994; Mészáros & Rees 1997; Panaitescu & Mészáros 1998; Sari & Piran 1999). However, the Waxman & Drain scenario has two shortcomings. First, the equilibrium temperature of dust is limited to ~2300 K, and so the emission should peak at ~$2(1 + z)$ μm (where z is the GRB redshift), although a small amount of higher temperature emission may be produced by the dust as it is subliming. Second,

the optical flash is so powerful that the sublimation radius lies beyond ~10 pc from the GRB. Thus, in this picture, it is rather difficult to reproduce the observed flux in the 0.4–0.8 μm band with a time delay of order a few weeks.

In this Letter, we propose an alternative explanation, which relies on the *scattering* of the direct optical transient emitted on the first day by dust as the primary source of excess optical radiation. The fundamental point is that in the two observed cases, assuming isotropic emission, the fluence of the *observed transient* exceeds that of the reported excess, and the *unobserved transient* is even larger if we extrapolate to earlier times. A fraction of this emission scattered from a radius where dust can outlive the optical transient should therefore produce a delayed echo. As dust absorbs selectively as well as scatters, the echo is likely to be significantly redder than the original optical transient, as reported.

In the next section, we describe our model for the dust scattering properties and then present the results in the context of the observed GRBs in § 3. Implications for future tests of our scenario are discussed in § 4. We assume $h = 0.6$, $\Omega_M = 0.3$, and $\Omega_\Lambda = 0.7$ so that the angular diameter distance of the GRB is $D_A = 1.5$–2 Gpc for $0.5 \lesssim z \lesssim 3$.

2. DUST ECHOES

2.1. *Sublimation Radius*

Waxman & Draine (2000) estimate that dust grains in the path of the optical/UV flash will be effectively sublimed out to a distance

$$R_{\rm sub} \sim 1(Q_{\rm abs}L_{47}/a_{-1})^{1/2} \ {\rm pc}, \qquad (1)$$

where $Q_{\rm abs} \sim 1$ is the absorption efficiency factor for optical/UV photons, $L_{47} \equiv \int d\nu \, L_\nu / 10^{47}$ ergs s^{-1} is the unbeamed luminosity of the optical transient (OT) in the 1–7.5 eV energy band, and $a_{-1} \sim 1$ is the dust grain size in units of 0.1 μm. Beyond $R_{\rm sub}$, only the most refractory grains, like silicates, can survive. Note that the thermal time for a typical dust particle is of order 10^{-4} to 10^{-2} s, much shorter than the duration of the optical transient, so that we can treat grains as being in thermal equilibrium with the incident radiation (which has a pressure $P_{\rm sub} \sim 0.03$ dyn cm^{-2} at $R_{\rm sub}$).

The extinction properties of silicate dust particles were computed by Draine & Lee (1984; see their Fig. 10), for a power-
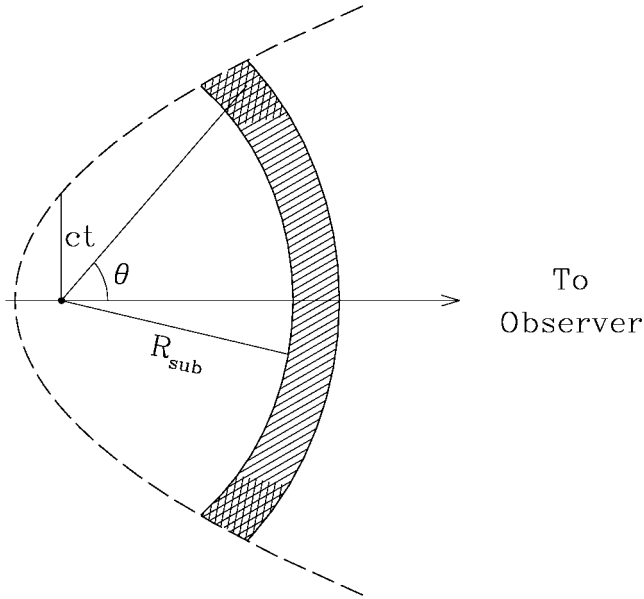
[1] Chandra Fellow.

FIG. 1.—Schematic diagram of the GRB environment. The long-dashed line represents the position of the expanding optical/UV photon front at time t in the frame of the GRB. The hatched/crosshatched area shows the region where the dust is not sublimated instantaneously. The crosshatched area shows the region of the shell from which the scattered radiation is observed, while the hatched area represents the regions where the dust is not scattering any more.

law distribution of particle sizes proposed by Mathis, Rumpl, & Nordsieck (1977) to explain interstellar starlight extinction. Based on their results, we take the ratio of the scattering and absorption efficiency factors to be of order $Q_{sc}/Q_{abs} \simeq 4$ and the average scattering angle to be $\langle \cos \theta \rangle \equiv \langle \mu \rangle \simeq 0.5$ for observed wavelengths 0.2–$1(1 + z) \mu$m.

2.2. Source Geometry

Figure 1 shows a schematic picture of the GRB environment observed at time t after the detection of gamma rays. The incident optical transient emission is supposed to be limited to an interval $\Delta t^{OT} \equiv \Delta t_{ob}^{OT}/(1 + z) \ll t$ after the GRB and scattered by dust beyond R_{sub}. We specialize immediately to the case when the dust is associated with an outflowing spherical wind and the OT is isotropic. (It is straightforward to modify our formalism to accommodate other reasonable assumptions, as discussed in Madau, Blandford, & Rees 1999.) Since the dust density declines with distance as R^{-2}, the light "echo" observed at time $t_{ob} = t(1 + z)$ will be scattered by dust concentrated in a ring located at the intersection of the sphere $R = R_{sub}$ and the paraboloid

$$t = \frac{R}{c}(1 - \mu), \tag{2}$$

where $\mu = \cos \theta$ (see Fig. 1). In our model, it is adequate to ignore a finite reprocessing time and the radial distribution of the dust. The dust only has to survive for a time $\sim \Delta t^{OT}$. We expect that, in practice, it will be quickly destroyed by the effects of secondary cosmic-ray electrons created through electron scattering of the GRB so that the observed optical afterglow need not necessarily be subject to the same extinction as the echo.
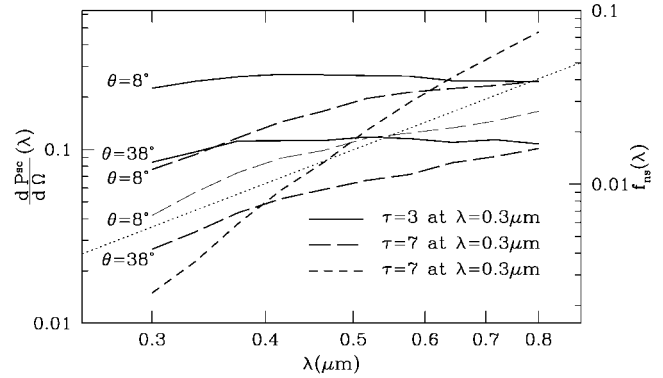

FIG. 2.—Solid and long-dashed lines show the escape probability for photons scattered by a dust slab for different values of θ and τ (as marked in figure). For comparison, the dotted line represents an escape probability that increases the spectral index of the echo relative to the OT by 2. The thin long-dashed line shows the results computed using a different $d\sigma/d\Omega \propto 1 + 2\mu + \mu^2$ which gives similar results although it is less peaked at $\mu \sim 1$. The short-dashed line shows the fraction of photons at each wavelength, $f_{ns}(\lambda)$, which pass through the slab unscattered, approximating the escape probability at $\theta = 0$.

2.3. Optical Scattering

The optical echo flux density $F_{\nu_{ob}}^E$, observed at frequency $\nu_{ob} = \nu(1 + z)^{-1}$, is

$$F_{\nu_{ob}}^E(\nu_{ob}, t_{ob}) = \frac{L_\nu(\nu, t)}{2(1 + z)^3 D_A^2} \frac{c\Delta t^{OT}}{R} \frac{d\mathcal{P}^{sc}}{d\Omega}(\nu, \mu),$$

$$0 < t_{ob} < 2R_{sub}(1 + z)/c, \tag{3}$$

where $d\mathcal{P}^{sc}(\nu, \mu)/d\Omega$ is the probability of escape along the direction defined by angle $\theta = \cos^{-1} \mu$ for a photon of frequency ν.

From equation (3), it is clear that the only time dependence comes from the angular dependence of the escape probability, $d\mathcal{P}^{sc}/d\Omega$; $F_{\nu_{ob}}^E(t_{ob})$ is simply a step function for isotropic scattering. We adopt a Henyey-Greenstein function (e.g., White 1979) to describe the differential cross section for dust scattering:

$$\frac{d\sigma}{d\Omega} \propto \frac{1 - \langle \mu \rangle^2}{(1 + \langle \mu \rangle^2 - 2\langle \mu \rangle \mu)^{3/2}}, \tag{4}$$

with $\langle \mu \rangle = 0.5$ (Draine & Lee 1984). We then use equation (4) to compute $d\mathcal{P}^{sc}(\lambda, \mu)/d\Omega$ numerically for a slablike dust cloud. The results for different observer angles (with respect to the slab normal vector) and two different values of the total extinction, $\tau = \tau_{abs} + \tau_{sc}$ (measured at $\lambda = 0.3 \mu$m) are shown in Figure 2. The differential escape probability is normalized so that the integral $\int_{4\pi}(d\mathcal{P}^{sc}/d\Omega)(\lambda, \mu)d\Omega$ is equal to the escape probability from the dust cloud. Figure 2 shows that at low optical depth, $\tau_{0.3} \equiv \tau(0.3 \mu$m$) \lesssim 3$, the echo should have a similar color to the OT, whereas at larger τ, the echo will be much redder due to absorption.

To illustrate that our calculation of the escape probability is not overly simplified (although it ignores wavelength dependence of the functional form for $d\sigma/d\Omega$; e.g., White 1979) in Figure 2 we show one curve (*thin long-dashed line*) computed using $d\sigma/d\Omega \propto 1 + 2\mu + \mu^2$. This expression gives the same value of $\langle \mu \rangle$ but is less strongly peaked at $\mu = 1$ than equation (4). The resulting $d\mathcal{P}^{sc}(\lambda, \mu)/d\Omega$ is very similar to what we use in our calculations.

The angular dependence of the escape probability is exhibited in Figure 3 for a dust cloud with $\tau_{0.3} = 7$ and three values of the incident photon wavelength. Note that $d\mathcal{P}^{sc}(\mu)/d\Omega$ remains relatively flat for $\theta \lesssim \theta_{sc} \sim 20°$ and decreases exponentially at larger angles.

2.4. Infrared Echo

Hot dust will also emit an isotropic infrared echo because of thermal emission from dust at the rapid sublimation temperature of ~ 2300 K, peaking at an observed wavelength $\lambda \sim 2(1 + z)$ μm. Waxman & Draine (2000) argue that only UV photons in the 1–7.5 eV range will contribute to dust heating. For $\tau_{0.3} \sim 7$, the absorption efficiency for photons in this energy range is greater than 0.8; moreover, such photons are likely to carry a considerable fraction of the total OT emission. Therefore, the integrated infrared flux is

$$F_{IR}^E = \frac{L\Delta t^{OT}}{8\pi D_A^2} \frac{c}{R} \frac{1}{(1+z)^4}. \tag{5}$$

3. COMPARISON WITH OBSERVATIONS

3.1. OT-Echo-Redshift Relations

Adopting our simple model of dust scattering, equations (1) and (2) allow us to relate the sublimation radius and OT power, $10^{47}L_{47}$ ergs s^{-1}, to the observed echo delay, $t_{ob}^E \equiv 10^6 t_{ob,6}^E$ s:

$$R_{sub} \sim 0.2 C_1^{-1} C_2^{-1} t_{ob,6}^E (1 + z)^{-1} \text{ pc}, \tag{6}$$

$$L_{47} \sim 0.03(1 + z)^{-2} C_1^{-2} C_2^{-2} (t_{ob,6}^E)^2, \tag{7}$$

where $C_1 = (1 - \mu)/0.06$ allows for beaming, or characteristic scattering angles different from 20°, and $C_2 = R/R_{sub}$ should be used if the dust is located beyond R_{sub}.

For simplicity, we now suppose that the spectral index of the OT is $\alpha \sim 1$. This is quite close to the spectral index of the observed afterglows. We can then use equation (3) to relate the R-band (0.65 μm) echo flux density to the escape probability

$$F_{\nu_{ob}}^E(0.65 \ \mu\text{m}) \sim 0.4 \frac{dP^{sc}}{d\Omega}(\nu, \mu) \left(\frac{t_{ob,6}^E \Delta t_{ob,3}^{OT}}{C_1 C_2^2}\right)$$

$$\times \left(\frac{D_A}{1.5 \text{ Gpc}}\right)^{-2} (1 + z)^{-6} \ \mu\text{Jy}, \tag{8}$$

where the observed duration of the optical transient is $10^3 \Delta t_{ob,3}^{OT}$ s. Note the strong dependence on redshift implying that accurate measurements of both the optical transient and the echo flux could lead to a fairly precise redshift prediction.

The ratios of the optical transient flux density, $F_{\nu_{ob}}^{OT} = L_\nu f_{ns}(4\pi)^{-1} D_A^{-2}(1 + z)^{-3}$, and infrared echo flux density to the optical echo flux density are likewise given by

$$\frac{F_{\nu_{ob}}^{OT}(0.65 \ \mu\text{m})}{F_{\nu_{ob}}^E(0.65 \ \mu\text{m})} \sim 3000 \left(\frac{f_{ns}}{C_1 \ dP^{sc}/d\Omega}\right) \left(\frac{t_{ob,6}^E}{\Delta t_{ob,3}^{OT}}\right); \tag{9}$$

$$\frac{F_{\nu_{ob}}^E[2(1 + z) \ \mu\text{m}]}{F_{\nu_{ob}}^E(0.65 \ \mu\text{m})} \sim 0.5 \left(\frac{dP^{sc}}{d\Omega}\right)^{-1} (1 + z), \tag{10}$$

where f_{ns} is the fraction of incident OT photons, emerging unscattered from the dust cloud.
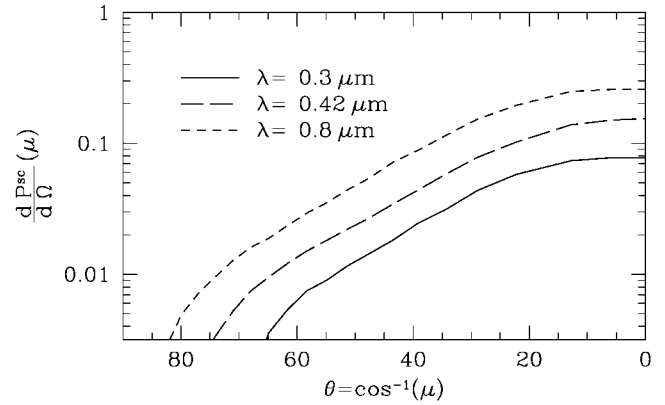

FIG. 3.—Differential escape probability plotted as a function of θ for a dust cloud with the optical depth for extinction $\tau_{0.3} = 7$. The results are shown for three different values of the incident photon wavelength.

3.2. GRB 980326

For GRB 980326, an excess R-flux $F_{\nu_{ob}}^E(0.65 \ \mu\text{m}) \sim$ 0.4 μJy was measured at time $t_{ob}^E \sim 20$ days (Bloom et al. 1999). If we make the simplest assumptions, $a_{-1} \sim Q_{abs} \sim C_1 \sim C_2 \sim 1$, then $R_{sub} \sim 0.3(1 + z)^{-1}$ pc and $L \sim 9 \times 10^{45}(1 + z)^{-2}$ ergs s^{-1}. Comparing the reported spectral slope ($\alpha \sim 2.8$) of the putative echo with that of the afterglow ($\alpha \sim 0.8$), we estimate that $\tau_{0.3} \sim 7$ (see Fig. 2). This in turn implies that $dP^{sc}/d\Omega$ in the observed R band is $\sim 0.2(1 + z)^{-1}$ and that $f_{ns} \sim 0.05(1 + z)^{-4}$ (see Fig. 2). We can then use equation (8) to deduce that $\Delta t_{ob,3}^{OT} \sim 3(1 + z)^7$ and $F_{\nu_{ob}}^{OT}(0.65 \ \mu\text{m}) \sim 200(1 + z)^{-10}$ μJy. If $z \sim 0.4$, then the energy associated with the first optical measurement of the afterglow ($F_{\nu_{ob}}^{OT}(0.65 \ \mu\text{m}) \sim 10$ μJy after 0.5 days) suffices to account for the observed excess after 20 days as a dust echo. If $z > 0.4$, then the optical transient would have had to be present and create a larger fluence at earlier times. This is not unreasonable since the afterglow flux was measured to satisfy $F^{OT} \propto t^{-2}$. In view of the large number of simplifying assumptions that we have made, this estimate can only be regarded as illustrative. However, it suffices to demonstrate that dust scattering is consistent with all of the available data.

3.3. GRB 970228

A somewhat similar story can be told for GRB 970228, where the redshift, $z = 0.695$, is known (Djorgovski et al. 1999). The earliest R-band measurement is ~ 30 μJy 0.7 days after the GRB; after ~ 30 days, there red excess flux of ~ 0.3 μJy was observed, with the spectral slope ($\alpha \sim 3.0$) very similar to that seen in GRB 980326 (Galama et al. 2000). For this object, again, within the uncertainties, the fluence measured in the first stages of the optical transient is sufficient to account for the energy in the optical excess.

3.4. Dust Origin

In both examples above, the mass of dust required to produce an optical depth $\tau_{0.3} \sim 7$ with our simplest assumptions, and assuming that it is spherically symmetrically distributed with respect to the GRB, is ~ 0.1 $M_\odot$. This amount of dust could form in an expanding high-metallicity wind associated with an earlier stage in the evolution of the GRB progenitor (see, e.g., Jura & Werner 1999), as we have assumed in our simple model. Alternatively, the dust might be associated with a molecular

cloud, if GRBs are associated with massive star formation, or a molecular torus, if they are located in obscured galactic nuclei.

4. DISCUSSION

In this Letter, we present an alternative explanation for the reddened excess emission observed in GRB 970228 and GRB 980326, which we attribute to dust scattering of the early-time, afterglow emission. This scenario is predictive enough to be confirmed or ruled out with observations of future GRBs. In particular, in contrast to the supernova explanation (Bloom et al. 1999; Reichart 1999; Galama et al. 2000), if the excess emission is due to dust scattering, then its properties will depend on the luminosity of the optical transient. *HETE-2*,[2] scheduled to be launched in early 2000, and *Swift*,[3] scheduled for 2003, should provide real-time localization of GRB X-ray afterglows with sufficient precision to permit faster follow-up and better measurements of their total fluence. Infrared observations show the expected thermal emission from hot subliming dust (see Waxman & Draine 2000). In fact, dust emission might be the correct explanation for the "near-IR" bump seen in the spectrum of the GRB 991216 afterglow (Frail et al. 2000). Note that since most GRBs are at redshifts $\gtrsim 0.5$, 3 μm (as opposed to the more common 2 μm), photometry may be necessary to see this emission.

In those GRBs, where it is possible to measure a redshift, the simplest model of dust scattering is overconstrained and

[2] See http://space.mit.edu/HETE/.
[3] See http://swift.gsfc.nasa.gov/homepage.html.

therefore refutable. Beaming and dust inhomogeneity introduce additional uncertainty, but such models may also be excludable. For example, if the Robotic Optical Transient Search Experiment (Akerlof et al. 1999) detects another optical flash in a GRB as luminous as that seen in GRB 990123, which had an isotropic luminosity $L \sim 10^{51}$ ergs s^{-1}, then dust should be physically sublimed out to a distance $R_{\rm sub} \sim 100$ pc along the line of sight. Unreasonably large beaming would then be required to explain a dust echo with a delay of only a few weeks. Alternatively, if the radio light curve in an afterglow tracked the optical light curve, then this would be incompatible with both dust scattering and a supernova.

A further prediction of the dust echo model is that, unless the dust and OT are both arranged axisymmetrically with respect to the line of sight, we expect there to be linear polarization associated with dust echoes, and this may be measurable in bright examples (1.7% polarization has been reported in the optical transient associated with GRB 990510 by Covino et al. 1999, but this is unlikely to be due to scattering).

In conclusion, we have demonstrated that dust scattering can account for the excess optical emission observed in the afterglows of two GRBs, as an alternative to an underlying supernova explosion. Future observations should be able to rule out or confirm this explanation.

REFERENCES

Akerlof, C. W., et al. 1999, GCN Circ. 205 (http://gcn.gsfc.nasa.gov/gcn/gcn3/205.gcn3)
Bloom, J. S., et al. 1999, Nature, 401, 453
Castander, F. J., & Lamb, D. Q. 1999, ApJ, 523, 593
Covino, S., et al. 1999, A&A, 348, L1
Djorgovski, S. G., et al. 1999, GCN Circ. 289 (http://gcn.gsfc.nasa.gov/gcn/gcn3/289.gcn3)
Draine, B. T., & Lee, H. M. 1984, ApJ, 285, 89
Frail, D. A., et al. 2000, ApJ, submitted (astro-ph/0003138)
Fruchter, A. S., et al. 1999, ApJ, 516, 683
Galama, T. J., Groot, P. J., van Paradijs, J., & Kouveliotou, C. 1998a, in AIP Conf. Proc. 428, 4th Huntsville Symp. on Gamma-Ray Bursts, ed. C. A. Meegan, R. D. Preece, & T. M. Koshut (New York: AIP), 478
Galama, T. J., et al. 1997, Nature, 387, 479
———. 2000, ApJ, in press (astro-ph/9907264)

Galama, T. J., et al. 1998b, Nature, 395, 670
Jura, M., & Werner, M. W. 1999, ApJ, 525, L113
Kulkarni, S. R., et al. 1998, Nature, 395, 663
Madau, P., Blandford, R. D., & Rees, M. J. 1999, ApJ, submitted (astro-ph/9912276)
Mathis, J. S., Rumpl, W., & Nordsieck, K. H. 1977, ApJ, 217, 425
Mészáros, P., & Rees, M. 1997, ApJ, 476, 232
Mészáros, P., Rees, M., & Papathanassiou, H. 1994, ApJ, 432, 181
Panaitescu, A., & Mészáros, P. 1998, ApJ, 501, 772
Reichart, D. E. 1999, ApJ, 521, L111
Sari, R., & Piran, T. 1999, ApJ, 520, 641
Waxman, E., & Draine, B. T. 2000, ApJ, submitted (astro-ph/9909020)
White, R. L. 1979, ApJ, 229, 954
Woosley, S. E. 1993, ApJ, 405, 273